Loop Strength of Spun Collagen Fibers

KAZIHIKO TAKAKU, TAKASHI KURIYAMA, and IKUO NARISAWA*

Department of Materials Engineering and Science, Yamagata University, College of Engineering, 4-3-16 Jonan, Yonezawa-city, 992, Japan

SYNOPSIS

The effects of gultaraldehyde (GA) crosslinking, basic chromium sulfate (Cr) tanning, and thermal treatments on the loop strength of spun collagen fibers were studied. The loop test have been carried out using a piano wire as a model loop. The promotion of GA crosslinking led a significant decrease of the strength and elongation at break. On the other hand, the promotion of Cr tanning gave no change. These properties decreased with an increasing shear stress at bending region of loop. The improvement of these mechanical properties were realized by thermal treatments of both GA crosslinked and Cr tanned fibers. The thermal treatment temperature showed the maximum effect at 100°C. However, there was no effect of thermal treatment for the noncrosslinked fibers. The fracture morphology of Cr tanned fibers is characterized by longitudinal splitting along the fiber axis in the bending region, although the fracture morphology of noncrosslinked and GA crosslinked fibers can be characterized by transverse fracture. © 1996 John Wiley & Sons, Inc.

INTRODUCTION

Spun collagen fibers have been tested as possible surgical sutures in the hope of making good use of this byproduct of the leather industry.[1-5] When the collagen spun fibers are used as a surgical suture, they are usually subjected to various loading stresses such as tensile, compressive, and/or bending stresses. In general, a knot test or loop test has been used as a practical test for many kinds of brittle fibers. For example, the results of the loop test for various kinds of material are reported in the literature.[6-11]

In these circumstances, it has been pointed out by Utsuo[1] that the knot strength of a spun collagen monofilament is insufficient to use as a surgical suture. It has been also reported by Taniguchi[3] that the crosslinking of spun collagen fibers leads to a decrease of knot strength. Although the knot strength of the spun collagen fibers has been studied, the fracture behavior and morphology of the spun collagen fibers subjected to the loop loading are not yet well understood.

The purpose of this paper is to study the influence of gultaraldehyde (GA) crosslinking, basic chromium sulfate (Cr) tanning, and thermal treatments on the fracture behavior and morphology under the loop test of the spun collagen fibers.

*To whom correspondence should be addressed.

Journal of Applied Polymer Science, Vol. 61, 2437–2445 (1996)
 CCC 0021-8995/96/132437-09

EXPERIMENTAL

As the preparation of the materials was described in detail in previous papers,[12,13] the experimental methods are only briefly described here.

Materials

A brine cured steer hide was soaked, limed, and unharied. The limed hide was delimed, rinsed, and cut and then the delimed corium pieces were alkaline treated, neutralized, and washed. The 6% collagen solution of pH 3.5 was prepared to spin. The spun fibers were obtained by wet spinning in acetone. Noncrosslinked fibers were obtained by treating the as-spun fibers at 100°C for 30 min under tension. The fibers of 0.1 wt %, 1.0 wt %, and 3.0 wt % GA crosslinked were obtained by treating the as-spun fibers. The fibers of 3.0 wt % and 7.0 wt % Cr tanned fibers were also obtained by the same method. After GA crosslinked and Cr tanning, they were washed, dehydrated by acetone, and dried at 100°C for 1 h under tension. Thermal treatments of noncross-

linked, 3.0 wt % GA crosslinked, and 7.0 wt % Cr tanned fibers were done in the dryer at 100, 140, and 170°C for 30 min under no tension. The mechanical tests were performed at 23°C and 65% RH after conditioning for 24 h. This conditioning resulted in the water content of the fibers is about 13 wt %.

Loop Test

A model loop test was carried out using piano wire and a UMT-4 tester (Toyo Sotuki Co. Ltd., Japan) with a cross-head speed of 10 mm/min. The diameters of the piano wire were 0.1, 0.2, and 0.3 mm. The loop tests of the fibers after thermal treatment were conducted by using only the piano wire of 0.1 mm in diameter. The loop test was done by forming a loop of 5 mm around the piano wire. Ten specimen pieces were used for each test. After the loop test, dried fibers were coated with a thin layer of gold and examined in a scanning electron microscope.

RESULTS AND DISCUSSION

Figure 1 shows the relationship between the half value of loop strength and the diameters D of the piano wire for GA crosslinked and Cr tanned fibers. They are compared with those of noncrosslinked fiber. Figure 2 shows that the similar relationship between the elongation at break and the diameters D of three piano wires. As clearly shown in Figures 1 and 2, the strength and elongation of each fiber increase with increasing D and finally they approach to the value of tensile strength. In other words, the strength and elongation of each fiber decrease with increasing shear stress at the bending region of the loop. The dependence of the strength of the GA crosslinked fibers on the concentration of a GA crosslinking agent gradually decreases with increasing D. Conversely, the dependence of the strength of the Cr tanned fibers on the concentration of a Cr tanning agent becomes large with increasing D. As shown in Figure 1(a), the strength of 0.1 wt % GA crosslinked fibers is approximately the same as those of noncrosslinked fibers, and the strength of 1 wt % and 3 wt % GA crosslinked fibers falls significantly for small loop diameters. As shown in Figure 1(b), the strengths of Cr tanned fiber are independent of the concentration of the Cr tanning agent. In Figure 2, the elongation at break of GA crosslinked fiber decreases with an increasing the concentration of the GA crosslinking agent, but the elongation of Cr tanned fibers was independent of the concentration of the Cr tanning agent. Although GA crosslinking

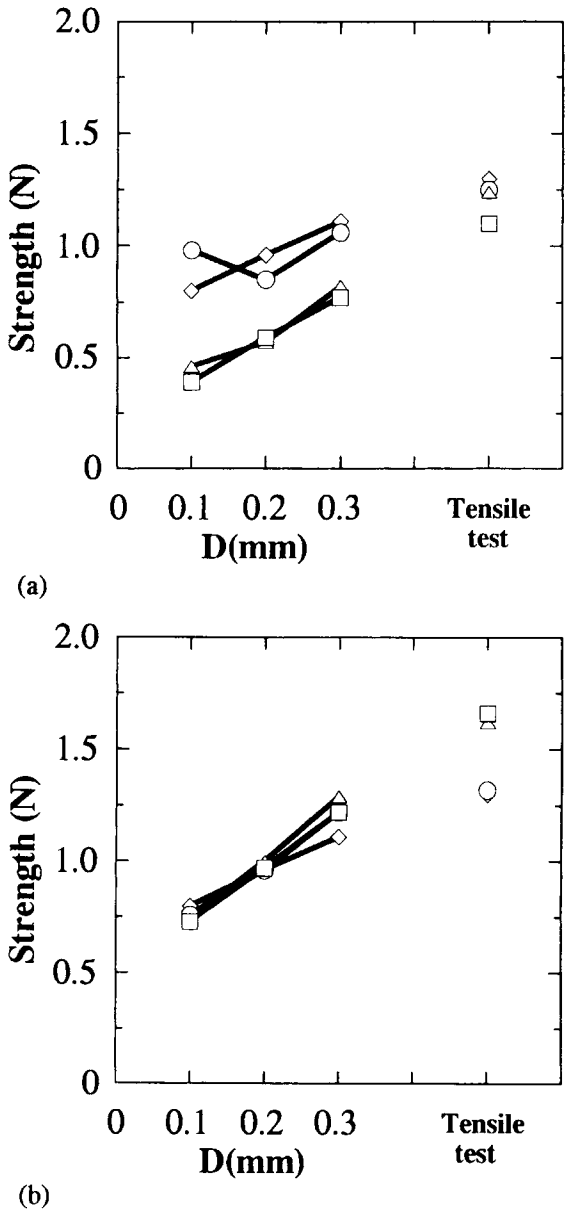

Figure 1 The relationship between loop strength and the diameter of piano wire for GA crosslinked (a) and Cr tanned (b) fibers. GA crosslinked fibers: ◇, noncrosslinked; ○, 0.1 wt % GA crosslinked; △, 1 wt % GA crosslinked; □, 3 wt % GA crosslinked. Cr tanned fibers: ◇, noncrosslinked; ○, 0.7 wt % Cr tanned; △, 3 wt % Cr tanned; □, 7 wt % Cr tanned.

and Cr tanning can improve the water resistance, the promotion of GA crosslinking results in an extreme decrease of the strength and elongation in the loop test. However, increases in Cr tanning have little affect on the loop strength and elongation.

Figures 3–5 show the results of scanning electron microscopy (SEM) observations of the fracture surfaces of non-crosslinked, 3 wt % GA crosslinked,

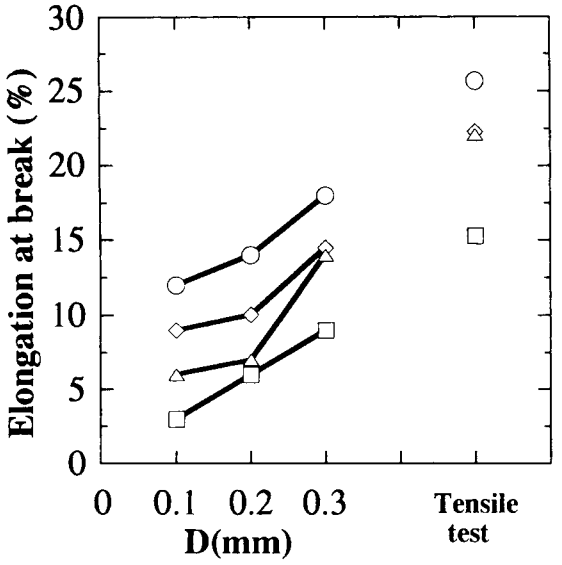

(a)

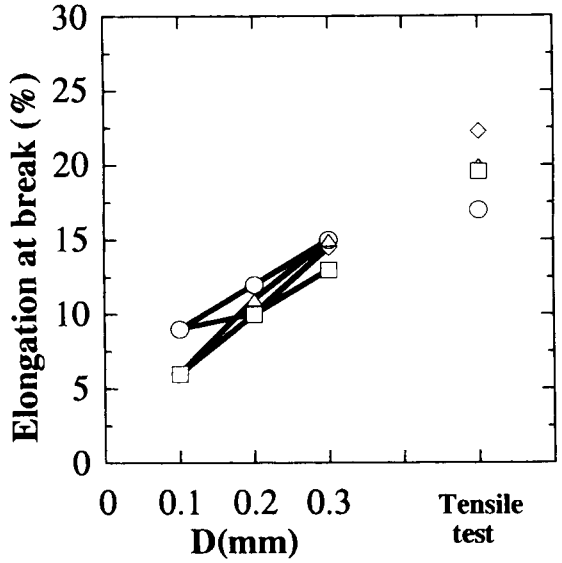

(b)

Figure 2 The relationship between the elongation at break and the diameter of piano wire for GA crosslinked (a) and Cr tanned (b) fibers. GA crosslinked fibers: ◇, noncrosslinked; ○, 0.1 wt % GA crosslinked; △, 1 wt % GA crosslinked; □, 3 wt % GA crosslinked. Cr tanned fibers: ◇, noncrosslinked; ○, 0.7 wt % Cr tanned; △, 3 wt % Cr tanned; □, 7 wt % Cr tanned.

and 7 wt % Cr tanned fibers. The fracture morphology of non-crosslinked and 3 wt % GA crosslinked fibers can be characterized by transverse fracture with a few and very short longitudinal splitting along the fiber axis. The fractured cross section in the bending region for non-crosslinked fibers shows the deformed region in which plastic deformation occurs in the bending region. The fracture morphology of GA crosslinked fibers can be characterized by brittle fracture surfaces. The frac-

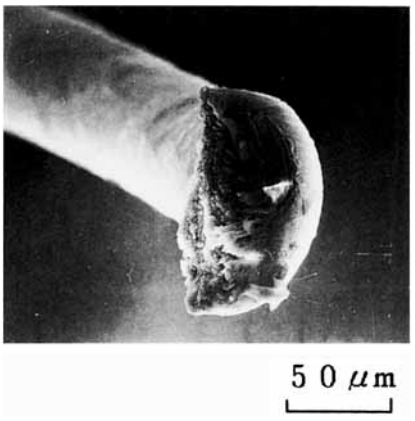

(a)

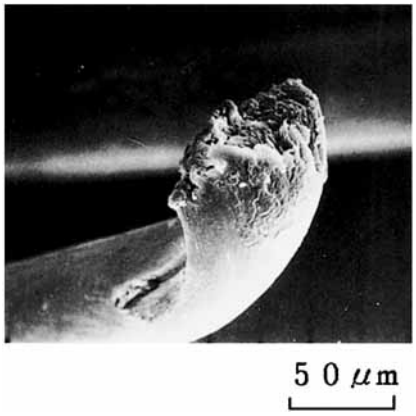

(b)

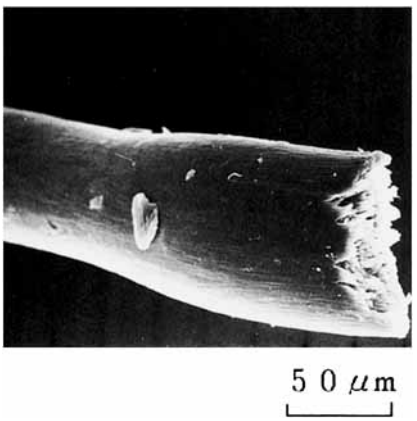

(c)

Figure 3 The SEM observations on the fracture surfaces of noncrosslinked fibers tested with piano wires of diameter (a) D = 0.1 mm, (b) D = 0.2 mm, and (c) D = 0.3 mm.

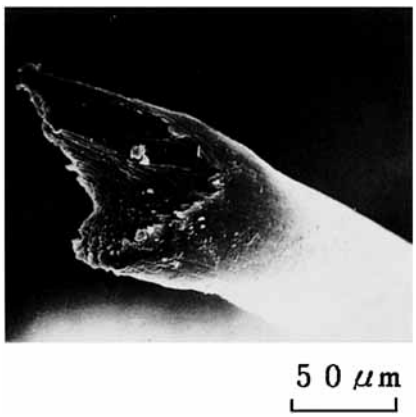

(a)

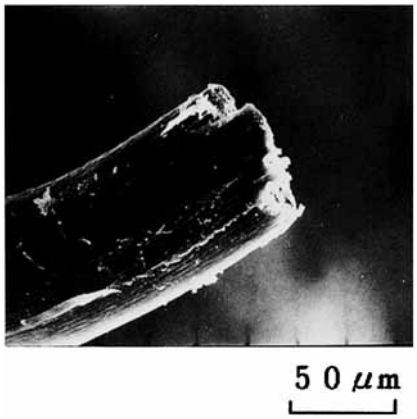

(b)

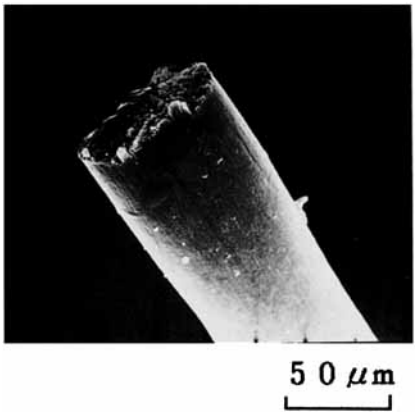

(c)

Figure 4 The SEM observations on the fracture surfaces of GA crosslinked fibers tested with piano wires of diameter (a) D = 0.1 mm, (b) D = 0.2 mm, and (c) D = 0.3 mm.

tured cross section in the bending region shows a circular shape. As shown in Figure 5, the fracture surfaces of Cr tanned fibers are characterized by many longitudinal splitting along the fiber axis in the bending region and the morphology of Cr tanned fibers is different from those of non-crosslinked and

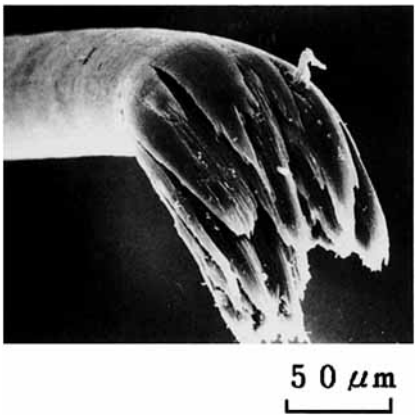

(a)

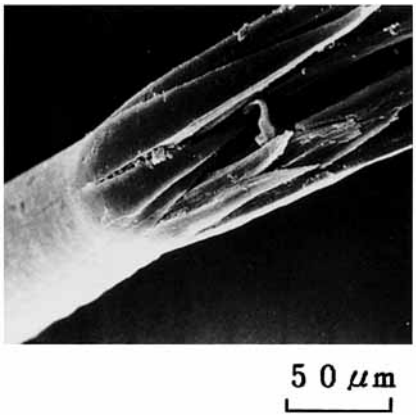

(b)

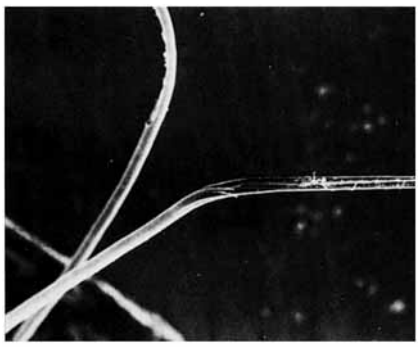

(c)

Figure 5 The SEM observations on the fracture surfaces of Cr tanned fibers tested with piano wires of diameter (a) D = 0.1 mm, (b) D = 0.2 mm, and (c) D = 0.3 mm.

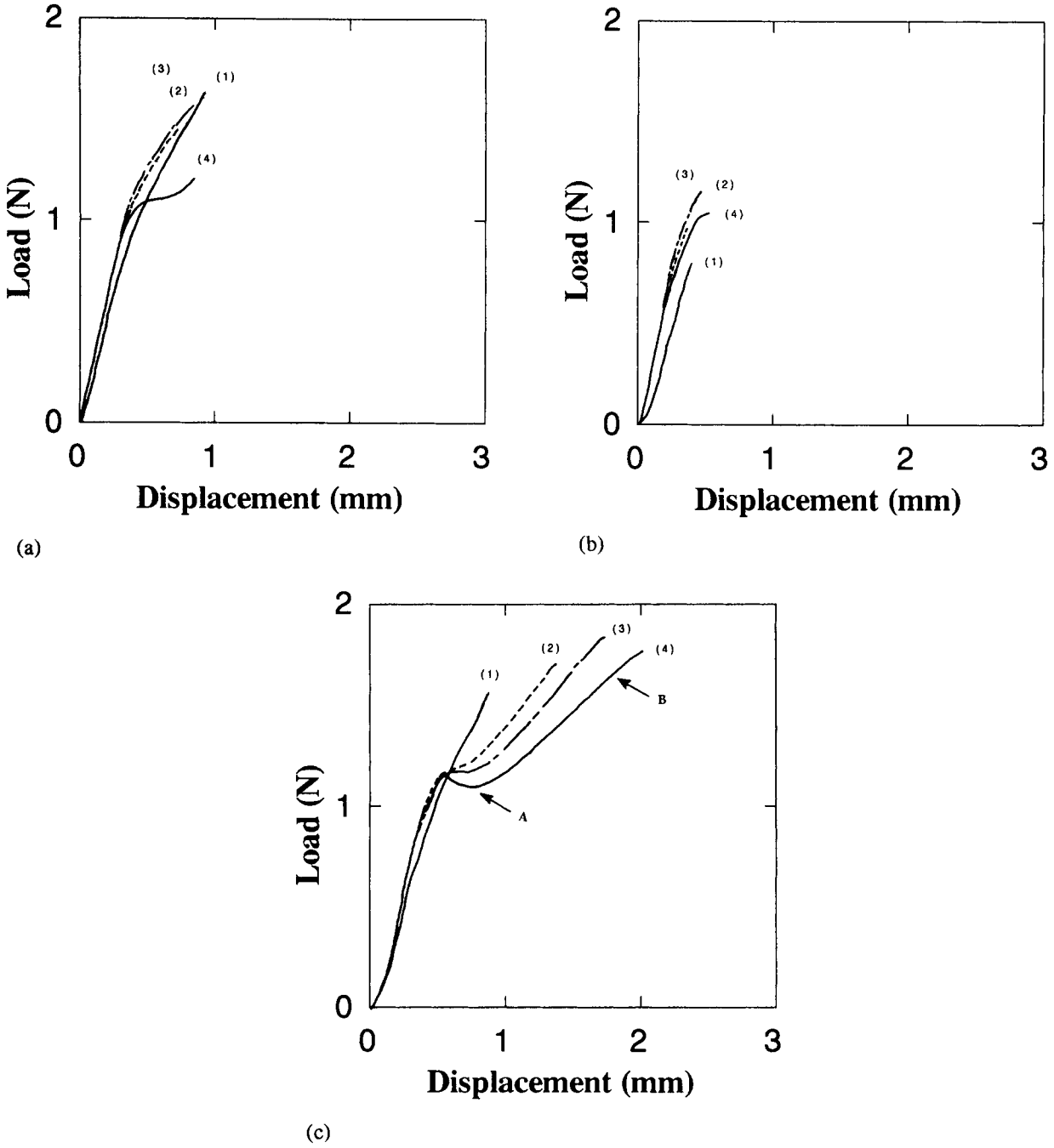

Figure 6 The typical load-displacement curves of noncrosslinked (a), 3 wt % GA crosslinked (b), and 7 wt % Cr tanned (c) fibers before and after thermal treatments. (1) Before thermal treatment. (2) After thermal treatment at 100°C. (3) After thermal treatment at 140°C. (4) After thermal treatment at 170°C.

GA crosslinked fibers. Another point of difference between the fracture morphology of noncrosslinked, GA crosslinked, and Cr tanned fibers is that the fracture region in noncrosslinked and GA crosslinked fibers at D = 0.3 mm is limited to the bending region in Figures 3(c) and 4(c), but for Cr tanned fibers the fracture occurs outside of the bending region as shown in Fig. 5(c). These results show that GA crosslinked fibers are more sensitive to bending stress than Cr tanned fibers.

As mentioned above, these results show that plastic deformation on the inner region of the loop of non-crosslinked fibers is the cause of the transverse cracking. Transverse fracture of GA cross-

linked fibers is caused by difficulty of fibril slippage along the fiber axis at the bending region. On the other hand, the longitudinal splitting of Cr tanned fibers is due to slippage between fibrils by shear stresses at the outer regions of the loop. The fracture morphology is therefore highly dependent on the kind of crosslinking. This is quite different from the results of tensile tests in which the fracture morphologies of the noncrosslinked, GA crosslinked, and Cr tanned fibers were nearly identical.[13]

The typical load-displacement curves of noncrosslinked, 3 wt % GA crosslinked, and 7 wt % Cr tanned fibers before and after thermal treatment are shown in Figure 6(a), (b), and (c), respectively.

As can be seen from Figure 6, the increase of thermal treatment temperature leads to give a clear knee point in the load-displacement curves of all kinds of fibers. The slope of the load-displacement curves of each treated fiber is larger than that of nontreated fibers. These results agree with the previous results in which tensile elastic modulus was increased by thermal treatments.[13] The load-displacement curves of Cr tanned fibers after thermal treatment are more similar to the tensile stress-strain curves after thermal treatment. The noncrosslinked and Cr tanned fibers treated at 170°C fracture after the knee point. The load increase after the knee point for Cr tanned fibers is more remarkable than that of noncrosslinked fibers. However, the fracture of GA crosslinked fibers occurs immediately after the knee point. Figures 7–9 show the SEM microphotographs of the fractured regions of noncrosslinked, 3 wt % GA crosslinked, and 7 wt % Cr tanned fibers that are treated at 170°C, respec-

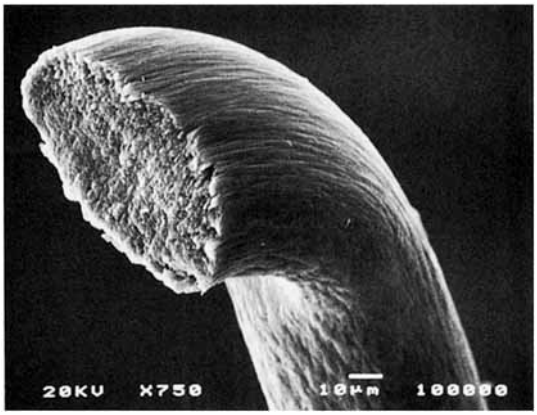

(a)

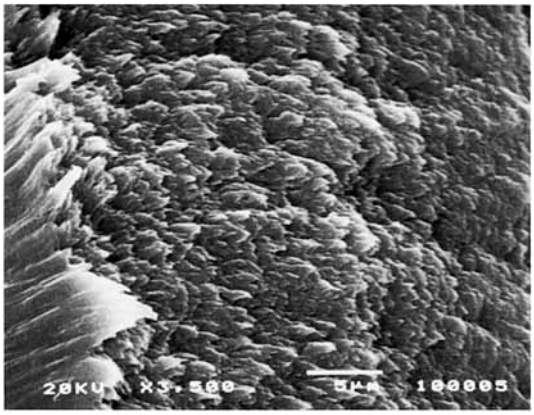

(b)

Figure 7 The SEM observations on the fracture surfaces of noncrosslinked fiber after thermal treatment at 170°C.

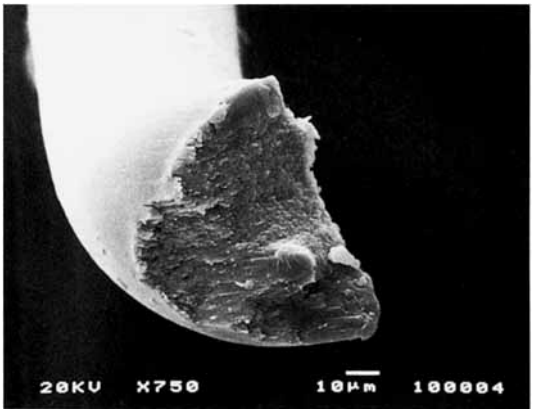

(a)

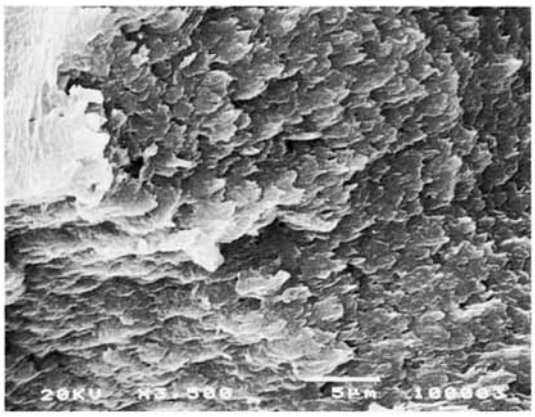

(b)

Figure 8 The SEM observations on the fracture surfaces of 3 wt % GA crosslinked fiber after thermal treatment at 170°C.

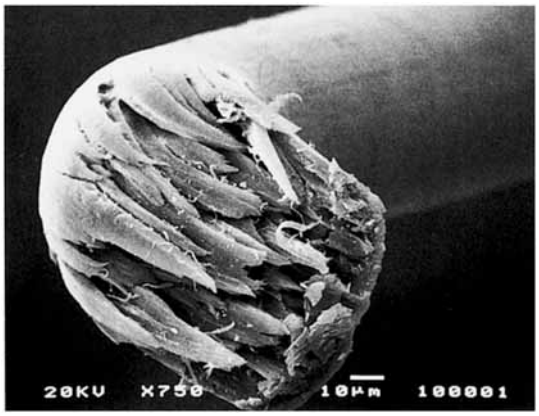

(a)

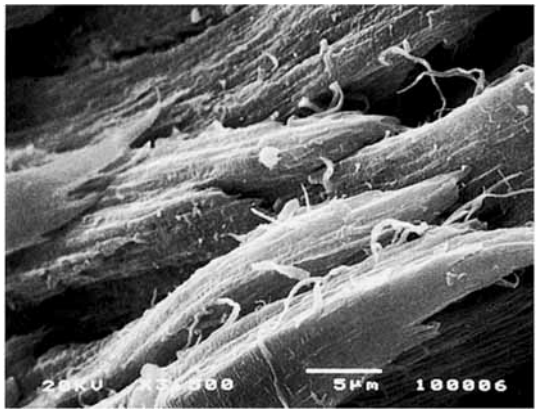

(b)

Figure 9 The SEM observations on the fracture surfaces of 7 wt % Cr tanned fibers after thermal treatment at 170°C.

tively. As shown in Figures 7(a), 8(a), and 9(a), the fracture surfaces of the noncrosslinked and GA crosslinked fibers is composed of a few and very short longitudinal splitted fibrils along the fiber axis. On the other hand, the fracture surface of the Cr tanned fibers shows many and long longitudinal splitting fibrils on the surface and inside of the fractured fiber. The lines, which have narrower intervals from 1 to 2 μm wide, are observed on the outer surface of the noncrosslinked fibers. However, these lines aren't observed on the outer surface of GA crosslinked fibers.

In Figures 7(b) and 8(b), many fibrils from 0.5 to 1 μm wide are observed on the cross-sectional surface of the noncrosslinked and GA crosslinked fibers. However, the fibrils of the noncrosslinked fibers are thinner than those of GA crosslinked fibers. Moreover, the many fibrils from 0.5 to 1 μm wide are observed on the longitudinal surface of the noncrosslinked fibers but are not observed on the surface of the GA crosslinked fibers. In Figure 9(b), the separated fibrils from 0.3 to 1 μm wide are observed in the region of longitudinal splitting of the Cr tanned fibers.

Figure 10(a) and (b) shows the SEM microphotographs of the outer bending surfaces of the 7 wt % Cr tanned fibers after thermal treatment at 170°C. They are corresponding to a point A above knee point on the load-displacement curve and to a point B just before break, respectively. In Figure 10(a), the lines of narrow intervals from 1 to 2 μm wide are observed on the outer surface at A point. In Figure 10(b), the longitudinal splitting initiates at the

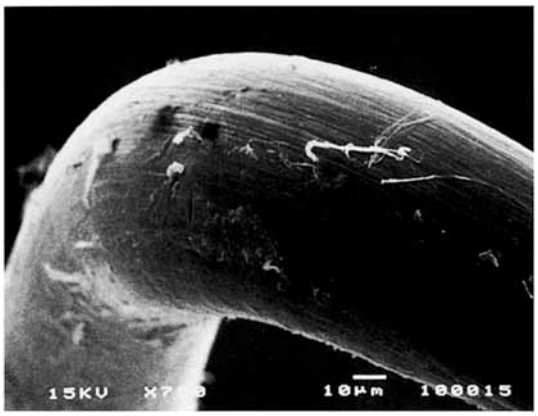

(a)

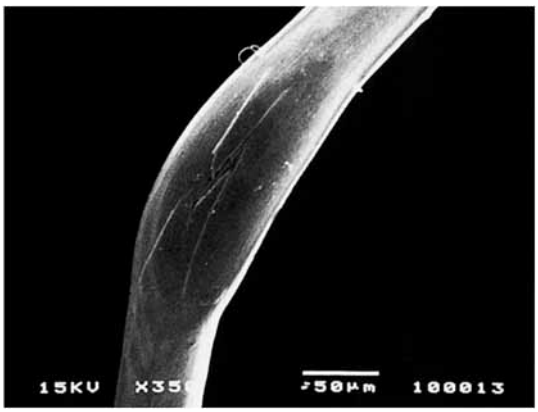

(b)

Figure 10 The SEM observations on the fracture surfaces of 7 wt % Cr tanned fibers after thermal treatment at 170°C. (a) A point A after knee point and (b) a point B before break.

center of the outer bending surface of bending region and it propagates from the center of bending toward the right and left directions along the fiber axis. The load-displacement curves of Cr tanned fibers after thermal treatment are much similar to the tensile stress-strain curves after thermal treatment, and the results of SEM observations show that the morphology after the knee points in the loop test is much similar to that after yield point in the tensile stress-strain curves.[13] Figures 9 and 10 show the process of longitudinal splitting of Cr tanned fibers. First, the longitudinal splitting takes place after fibril slips in the outer regions and then the longitudinal split initiates at the outer regions. Second, the longitudinal split propagates from the center of outer bending surface toward right and left directions along the fiber axis and then propagates inward throughout the original compressive zone. Finally, fracture occurs by the long longitudinal splitting as similar as fracture in the tensile tests.

As mentioned above, the fracture morphology of Cr tanned fibers before and after thermal treatment is characterized by many longitudinal splits along the fiber axis in the bending region and the longitudinal splitting does not depend on the loop diameter D. On the other hand, the fracture morphology of noncrosslinked and GA crosslinked fibers can be characterized by transverse cracking with a few and very short longitudinal splitting fibrils. The morphology of the transverse fracture of the noncrosslinked and GA crosslinked fibers also do not depend on the loop diameter D.

Figure 11(a) shows that the relationship between the loop strength and thermal treatment temperature for the noncrosslinked, 3 wt % GA crosslinked, and 7 wt % Cr tanned fibers. The loop strength is estimated by the loop strength divided by the cubic of the diameter because the diameter of each fiber is changed by thermal treatments. It is also known that the bending stress is inversely proportional to the cubic of diameter. Figure 11(b) shows the relationship between the elongation at break and thermal treatment temperature for the non-crosslinked, 3 wt % GA crosslinked, and 7 wt % Cr tanned fibers.

As shown in Figure 11(a), the loop strength of each fiber decreases with increasing treated temperature. Thermal treatments hardly improve the loop strength of the noncrosslinked fibers but enhance the loop strength of the GA crosslinked and Cr tanned fibers and give the maximum improving effect at 100°C. This is corresponding to the effect of thermal treatments on the tensile strength as shown in previous paper.[13] In Figure 11(b), the

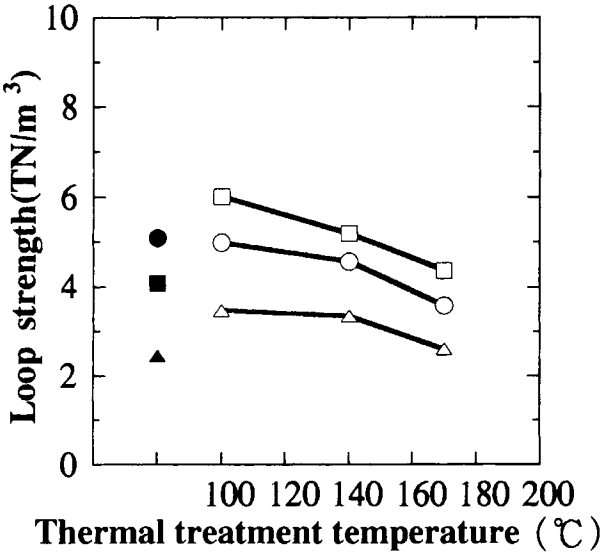

(a)

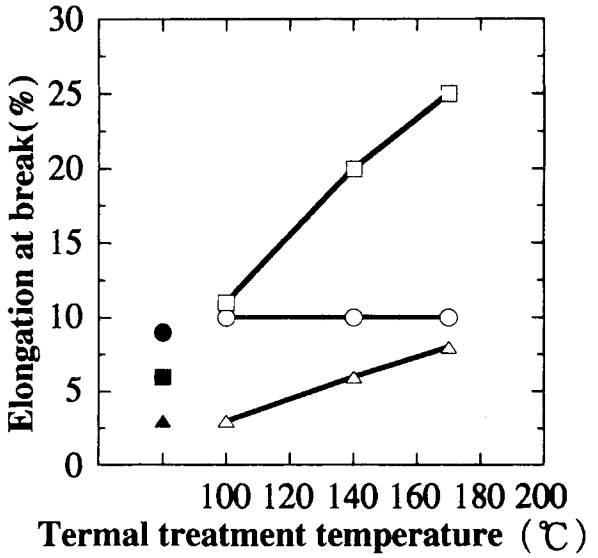

(b)

Figure 11 The influence of thermal treatment temperature on the loop strength (a) and elongation at break (b) for noncrosslinked, 3 wt % GA crosslinked, and 7 wt % Cr tanned fibers. Before thermal treatment: ●, noncrosslinked; ▲, 3 wt % GA crosslinked; ■, 7 wt % Cr tanned. After thermal treatment: ○, noncrosslinked; △, 3 wt % GA crosslinked; □, 7 wt % Cr tanned.

elongation at break of the GA crosslinked and Cr tanned fibers increases with increasing temperature. The increase of elongation of Cr tanned fiber is more remarkable than that of GA crosslinked fibers. The elongation of the noncrosslinked remained unchanged by thermal treatments.

CONCLUSIONS

The loop strength and elongation at break of noncrosslinked, GA crosslinked, and Cr tanned fibers increase with increasing bending diameter, namely those properties decrease with an increasing shear stress component in the bending region. The GA crosslinked fibers are more sensitive to bending stress than are the Cr tanned fibers. Increasing levels of GA crosslinking result in extreme decreases in strength and elongation. On the other hand, increasing levels of Cr tanning have little effect on these properties. Thermal treatment is effective for improving the loop strength and elongation of the GA crosslinked and Cr tanned fibers. Maximum improvement is obtained at 100°C. Thermal treatments do not enhance the loop strength of noncrosslinked fibers. It is thus shown that the effect of thermal treatment on the loop strength and elongation depends on the presence of crosslinks. The fracture morphology depends on the kind of crosslink and independent of the loop diameter and thermal treatment temperature. The fracture morphology of the Cr tanned fibers is characterized by many and long longitudinal splitting fibrils along the fiber axis in the bending region.

On the other hand, the fracture morphology of the noncrosslinked and GA crosslinked fibers are characterized by the transverse cracking with a few and very short longitudinal splitting fibrils. The results of SEM observations on the Cr tanned fibers show that the process of the longitudinal splitting is as follows. First, the longitudinal splitting occurs by fibril slippage by shear stress in the outer region of the bending fiber, and the longitudinal splitting initiates in the outer regions. Second, the longitudinal splitting propagates from the center of outer bending surface toward right and left directions along the fiber axis, and it grows inward throughout the original compressive zone. Finally, the fracture takes place with the long longitudinal splitting as similar as tensile fracture. On the other hand, plastic deformation on the inner region of bending fibers is the cause of the transverse cracking for the noncrosslinked fibers and the transverse fracture of GA crosslinked fibers results from the absence of fibril slippage. The fracture morphology of noncrosslinked and GA crosslinked fibers depends on the loading conditions. The fracture morphology of Cr tanned fiber independs on the loading conditions, and the fracture morphology in both loop and tensile tests is characterized by the longitudinal split along the fiber axis.

REFERENCES

1. A. Utsuo, *J. Textile Mach. Soc. Japan,* **26,** 207 (1973).
2. A. Utsuo, *Hikaku Kagaku (Jap.),* **20,** 209 (1975).
3. M. Taniguchi, *Kobunshi,* **12,** 608 (1963).
4. W. C. Schimpt and F. Rodriguez, *Ind. Eng. Chem., Prod. Res. Dev.,* **16** (1977).
5. F. Rodriguez, *Polymer News,* **9,** 262 (1984).
6. A. Konda and C. Koyama, *Bull. Textile Res. Inst. Japan,* **56,** 17 (1960).
7. A. Konda, T. Koyama, and T. Agatsuma, *Bull. Textile Res. Inst. Japan,* **59,** 17 (1961).
8. A. Konda, C. Koyama, and T. Agatsuma, *Bull. Textile Res. Inst. Japan,* **62,** 25 (1962).
9. A. Konda, H. Ishikawa, and K. Shirakashi, *J. Textile Mach. Soc. Japan,* **25,** 67 (1972).
10. A. Konda, T. Misaizu, and S. Sekiguchi, *J. Textile Mach. Soc. Japan,* **30,** 55 (1977).
11. M. G. Dobb, D. J. Johnson, and B. P. Saville, *Poymer,* **22,** 960 (1981).
12. S. Nakazaki, K. Takaku, M. Yuguchi, H. Edamatsu, and K. Takahashi, *Anim. Sci. Technol.* **65,** 1018 (1994).
13. K. Takaku, T. Ogawa, T. Kuriyama, and I. Narisawa, *J. Apply. Polym. Sci.,* **59,** 887 (1996).

Received September 27, 1995
Accepted April 9, 1996